Article

A global timekeeping problem postponed by global warming

https://doi.org/10.1038/s41586-024-07170-0

Received: 4 August 2023

Accepted: 6 February 2024

Check for updates

Duncan Carr Agnew[1]✉

The historical association of time with the rotation of Earth has meant that Coordinated Universal Time (UTC) closely follows this rotation[1]. Because the rotation rate is not constant, UTC contains discontinuities (leap seconds), which complicates its use in computer networks[2]. Since 1972, all UTC discontinuities have required that a leap second be added[3]. Here we show that increased melting of ice in Greenland and Antarctica, measured by satellite gravity[4,5], has decreased the angular velocity of Earth more rapidly than before. Removing this effect from the observed angular velocity shows that since 1972, the angular velocity of the liquid core of Earth has been decreasing at a constant rate that has steadily increased the angular velocity of the rest of the Earth. Extrapolating the trends for the core and other relevant phenomena to predict future Earth orientation shows that UTC as now defined will require a negative discontinuity by 2029. This will pose an unprecedented problem for computer network timing and may require changes in UTC to be made earlier than is planned. If polar ice melting had not recently accelerated, this problem would occur 3 years earlier: global warming is already affecting global timekeeping.

Many activities, such as communications, network computing, positioning and financial markets[6], require a consistent, standardized and precise timescale. This is now provided by Coordinated Universal Time (UTC), created by international coordination and used everywhere[1]. In UTC, the unit of the timescale is the second, defined by a physical oscillator (caesium atoms). The history of horology shows that oscillator-based definitions (before 1940 from pendula) have been used in almost all timescales in the past few centuries, whether the time was distributed by the bells of a turret clock[7,8], time balls[9], telegraphy[10,11] or radiowaves[12,13]. All such timescales have also included rules that coupled the timescale to the rotation of Earth, either by changing the oscillator frequency (in horological parlance changing the rate) or by introducing a discontinuity (resetting the clock).

Before 1955, any high-quality timescale had to be coupled to the rotation of Earth because this was more stable than any available oscillator, so the second was defined as a specified fraction of the time Earth took to rotate once relative to the stars. A count of these rotational seconds produced a timescale labelled UT1. Atomic frequency standards based on caesium are so much more stable than the rotation of Earth that the first paper announcing a working caesium oscillator was immediately followed by one[14] suggesting that this frequency be used to define a 'physical second'. A timescale using such seconds was established in 1955, and subsequent work[15,16] created, within a few years, an atomic timescale labelled TAI. UT1 and TAI were defined to agree on 1 January 1958; since then they have diverged because the Earth spins at a variable rate. This variability has complicated UTC in the past and seems likely to do so even more in the near future.

Causes of spin-rate changes

Taking the viewpoint that[17] 'the Earth is a geophysical laboratory, not a timekeeper', we specify its spin rate as the time-varying angular velocity, $\omega_s(t)$, of its solid part (the mantle and crust). We describe variations in ω_s by the normalized difference from a reference value ω_0: $\Delta_\omega = (\omega_s - \omega_0)/\omega_0$. (We use subscripted Δs throughout to designate the normalized differences.) Integrating Δ_ω from 1958 onwards gives the difference between UT1 and TAI.

Changes in Δ_ω occur because of the conservation of angular momentum, which for the solid Earth is $C_s\omega_s$, C_s being the moment of inertia of this part about the polar (spin) axis. This angular momentum is connected to the total angular momentum of the Earth, H, by

$$C_s\omega_s = H - [C_a\omega_a + C_w\omega_w + C_c\omega_c], \quad (1)$$

where the three terms in brackets are the angular momenta of the fluid parts of Earth: the first and second represent the air and the water above the solid part, and the third the (mostly fluid) core within it. Each of these parts has its own moment of inertia C and mean angular velocity ω. Variations in Δ_ω, and hence in UT1, can be caused by changes in any of the other variables; because TAI-UT1 is the integral of Δ_ω, longer-period changes have the most effect on this difference. Rewriting equation (1) as

$$\omega_s = H/C_s - [r_a\omega_a + r_w\omega_w + r_c\omega_c] \quad (2)$$

shows the relative importance of the other angular velocities. As $r_a = C_a/C_s = 1.5 \times 10^{-6}$; r_w is 5×10^{-4} and r_c is 0.13, changes in ω_c are

[1]Institute of Geophysics and Planetary Physics, Scripps Institution of Oceanography, University of California San Diego, La Jolla, CA, USA. ✉e-mail: dagnew@ucsd.edu

much more important than similar changes in ω_a and ω_w. A motion of 1 m s^{-1} in the atmosphere and 30 m yr^{-1} in the core alter ω_s by the same amount.

For periods between a few days and a few years, most of the change in ω_s comes from two sources. The first is changes in $C = C_s + C_w + C_c$ as the Earth is deformed by the tidal forces from the Moon and Sun. Most of these tidal-deformation changes cause UT1 variations of a few milliseconds, although one UT1 variation has a period of 18.6 years and an amplitude[18] of 0.18 s. The second source is changes in $C_a\omega_a$ and $C_w\omega_w$ related to atmosphere and ocean motions, with the largest contribution[19] from changes in ω_a. Seasonal changes in C_a and ω_a cause UT1 to vary by about 0.025 s. Spectral analysis shows that nonseasonal variations in these terms (also dominated by changes in ω_a) are the largest contributor to changes in Δ_ω for periods from days to about 5 years. The variations in Δ_ω induced by atmosphere and ocean motions are close to white noise, creating a random-walk variation in UT1 of less than ±0.3 s in the past 50 years.

Tidal forces also apply a torque to the whole Earth, reducing H and hence ω_s: this is known as tidal friction. On the time scales treated in this paper, the ocean tides are essentially constant[20] and the tidal friction diminishes ω_s at a constant rate. Measurements of lunar motion[21] show that tidal friction causes Δ_ω to change by -2.77×10^{-10} yr^{-1}.

Another cause of steady changes in ω_s is the decrease in C_s from the continued readjustment of Earth following the melting of the ice caps that covered the Canadian Arctic and Fennoscandia. This readjustment, termed glacial isostatic adjustment (GIA)[22,23], does vary over millennial timescales, but over centuries it steadily makes the Earth more spherical, causing Δ_ω to change by about[24,25] 0.9×10^{-10} yr^{-1}.

Because tidal friction and GIA cause a quadratic variation in TAI-UT1, the sum of these has tended to dominate the predictions of this difference[26]. But changes in C_w and ω_c must also be considered; when they are, recent and near-term changes in UT1 can be seen to be affected by them in consequential ways.

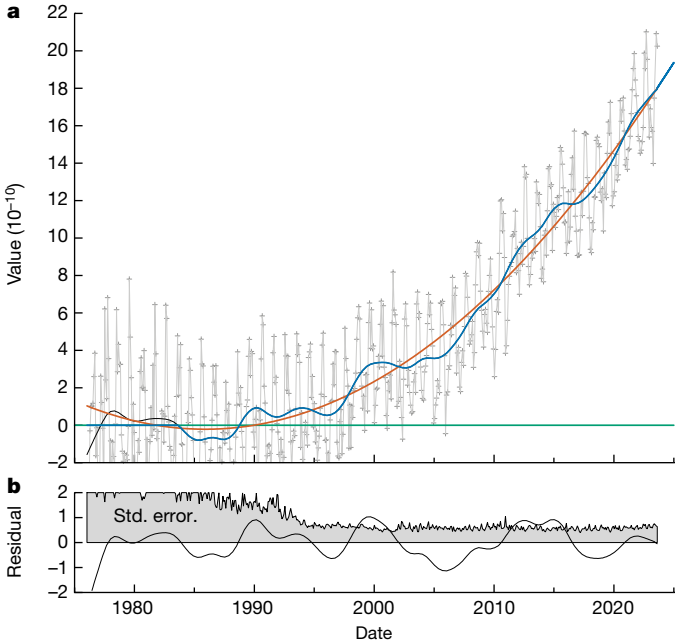

Fig. 1 | Changes in J_2. a, Monthly variations in J_2 estimated from satellite tracking[27], with the trend to 1991 removed. The original values are in grey. The blue line is part of the correction applied to ω_s: zero before 1983.6, from 1983.6 to the end of the data it is the values obtained by seasonal adjustment and smoothing. The red curve is a quadratic fit to the smoothed and adjusted data, given by $0.128 \times 10^{-11} t^2$, where t is years from 1985.9; the blue line follows this after the end of the data. The green line is an alternate version of $J_2(t)$ with no acceleration.

Recent changes in spin caused by ice and iron

Changes in C_w can best be found by measuring the total moment of inertia $C = C_s + C_w + C_a$ and correcting for changes in C_s and C_a. C is proportional to one term in the spherical harmonic expansion of the gravity field of Earth, denoted by J_2, so its changes can be measured to high accuracy by tracking satellites[4,5,27]. Changes in J_2 because of redistribution of mass on the surface of Earth scale[19] to changes in ω_s as $\Delta_\omega = -1.7\delta J_2$.

Figure 1 shows the longest series of J_2 available from satellite measurements. The rate from 1976 to 1991, -0.35×10^{-10} yr^{-1}, has first been removed; this is the sum of -0.54×10^{-10} yr^{-1} from GIA-induced changes in C_s and 0.19×10^{-10} yr^{-1} from changes in C_w caused by ice near the poles melting with the water distributed over the oceans[25,28]. This process is part of the twentieth-century sea-level rise and is termed present-day mass transfer (PDMT). For melting or freezing in high latitudes, a change in 10^{-10} in J_2 corresponds to about a 2.3-mm change in sea level[29].

After seasonal adjustment, this J_2 time series shows an accelerating rate of change; fitting a parabola gives a departure from zero around 1986, extending behaviour noticed as early as 2002 (refs. 30,31) but now much clearer. The parabolic fit gives a current rate of 10^{-10} yr^{-1}, closely corresponding to the estimates of the current rate of sea-level change from added ocean mass[32,33].

Figure 2a–c shows how this increased rate of change in C_w compares with other sources of change in Δ_ω. Figure 2a shows the observed changes in Δ_ω starting in 1962 (when the necessary data became available), after removing changes from the tidal-deformation and atmosphere and ocean motions contributions. The remaining Δ_ω is a smooth, irregular and declining curve with ω_s increasing over the past 50 years. Currently, Δ_ω is close to zero, meaning that ω_s is close to the value assumed when the atomic second was defined; for complicated historical reasons[1,16,34], the TAI second is approximately the average value of the UT1 second between 1750 and 1892.

Figure 2b shows the contributions to Δ_ω of tidal friction, GIA and the PDMT inferred from J_2 changes (blue, to match Fig. 1); all have been set to be zero (grey line) in 1972. The contribution from PDMT without the recent acceleration is also shown (green; see Fig. 1). These contributions all have been extended as predictions to 2045, something easily done for tidal friction and GIA. Extrapolating the parabola in Fig. 1 gives a change supported by other predictions: from 2014 to 2050, it corresponds to 0.11 m of sea-level change, closely matching one prediction of the Sixth IPCC Report[32].

Figure 2c shows Δ_ω (ω_s) when these known contributions are removed from the observed values in Fig. 2a: this can be thought of as a 'Residual' part of changes in the spin of Earth. The acceleration of PDMT after 1987 lowers the last part of this curve, so that from 1972 to the present it is reasonably well approximated by a linear trend.

In terms of equations (1) and (2), changes in H, $C_a\omega_a$, $C_w\omega_w$ and C_s are fully accounted for, and the J_2 data rule out changes in C_c; so the only possible source for changes in the residual series is changes in ω_c (which do not affect J_2). We know that motions in the fluid core exist and produce variations of the magnetic field of Earth[35,36]. A spectral analysis[37] of the series in Fig. 2c shows that at periods longer than 3 years the power spectrum varies with frequency f as f^β with $\beta = -2.4$. For periods from a few years to centuries, the spectrum of the axial dipole of the magnetic field of Earth increases similarly but[38] with $-6 \le \beta \le -4$.

Measurements of Δ_ω over the past 200 years show even larger irregular changes[39], consistent with a very red spectrum for Δ_ω: although these changes are sometimes called decadal, they become even larger at longer periods and can be modelled as a stochastic process[40]. Core motions have been invoked to explain why the long-term rate from GIA and tidal friction, -1.85×10^{-10} yr^{-1}, might differ from the long-term rate of -2.00×10^{-10} yr^{-1} deduced from ancient eclipse records[24,41].

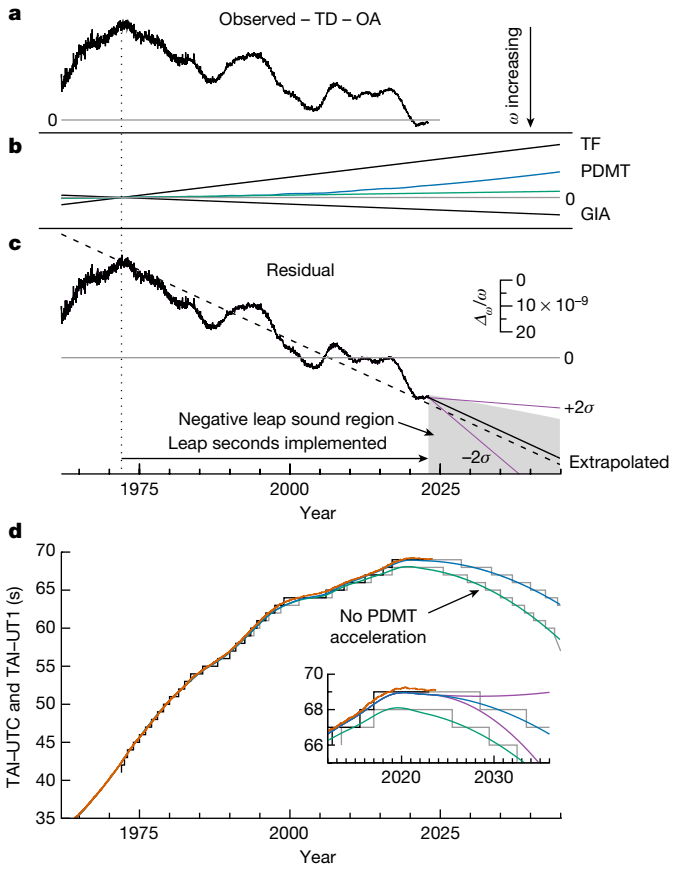

Fig. 2 | Changes in spin rate and their effects on timescales. a–**c**, Observations and causes of long-term changes in the nondimensionalized spin rate (Δ_ω) of Earth. Values increase downwards to match the plots of changes in the excess length of day. **a**, Observed daily values (after removal of known causes of short-term changes) are plotted. TD, tidal deformation; OA atmosphere and ocean motions. **b**, Spin-rate changes produced by tidal friction (TF), PDMT inferred from the J_2 changes shown in Fig. 1 and postglacial rebound (GIA). **c**, The series obtained by subtracting the effects in **b** from the observation in **a**. The dashed line is a fit to this residual series between 1972 and the end of the series in **a**. The black line shows an extrapolation from the end of the residual series with the same slope. **d**, The result of summing the past and future series in **b** and **c** and integrating them to get change in Earth orientation, expressed as time. Black and grey step functions show how this would translate into UTC, with steps (leap seconds). The blue and green lines correspond to the different choices for PDMT; the purple lines correspond to different extrapolations of the residual series in **c**. As the sum of residual, GIA, PDMT and tidal friction series matches the data in **a**, its integral (the blue line in **b**) closely matches (and is nearly hidden by) the observed TAI-UT1 (red). The green line shows the TAI-UT1 difference that would have happened if PDMT had not accelerated; the grey line around it shows an alternate UTC.

Future spin, UTC and leap seconds

Extrapolating the series in Fig. 2b,c provides a look into the near future of spin and timekeeping, which, because of the history of the UTC timescale[3,15] can vary substantially for even small changes in spin rate. The history of UTC began with coordinated time broadcasts that began in 1960; the rules for these, formalized in 1963, initially combined the annual changes in rate with occasional offsets of 0.1 s to track a seasonally corrected version of UT1.

In the 1960s, celestial navigation was widely used, both at sea and in the air, and the navigational community wanted a broadcast time tied, as it previously had been, to Earth rotation. But the even larger community involved with radio and other telecommunications methods wanted broadcasts to have a stable frequency. So in 1972, the rules for producing UTC (so named in 1967) were changed to maintain a constant frequency: in timekeeping terms, the length of the second was invariant. But 1-s discontinuities were to be applied as needed to keep UTC within 0.5 s of UT1. By the 1960s, Earth was and had been decelerating, and so rotating more slowly than in the nineteenth century, which defined the atomic second. In 1969, Δ_ω was about -3.2×10^{-8}, making the UT1 day about 2.8 ms longer than the TAI day. Over a year, UTC (tied to TAI) would then be 1 s behind UT1, so 1 s would be added to UTC: a 'leap second' discontinuity. Figure 2d shows that leap seconds were at first needed almost annually (23 times between 1972 and 1999); but there have been only four in the past 23 years. This change occurred because the slowing of the core has caused the solid Earth to rotate more rapidly: Δ_ω is now close to zero and the length of the day back to its nineteenth-century value.

Extrapolating the series in Fig. 2c by fitting a straight line predicts that Δ_ω will continue to increase. Figure 2c shows how this affects the predicted TAI-UT1: it starts to decrease so that before the end of this decade a second would need to be removed from UTC. This 'negative leap second' will be needed if the extrapolated series in Fig. 2c stays within the shaded region. Two extreme cases are given by varying the straight-line extrapolation by twice the standard error of its estimated value (purple lines): in one case, the negative leap second is needed in 2026 (Fig. 2d, inset), and at the other extreme it never occurs, with no positive leap second until 2040. The upper line approximates what would occur if the core continued to slow at a constant rate but ice melting was 100 times its current rate.

The consequences of a negative leap second, and the possible remedies for it, are affected by changes that have greatly altered the costs and benefits of the current rules for UTC since 1972. Celestial navigation is no longer a primary or even secondary method of positioning[42]. Computer timekeeping and networking, nonexistent in 1972, is now ubiquitous, and is based on counting seconds; there is no way to insert (or remove) a 'leap integer'[43]. The unpredictability of leap seconds makes it challenging to synchronize a vast global infrastructure. Different web services currently handle leap seconds differently[2]. Many systems now have software that can accept an additional second, but few if any allow for removing a second, so that a negative leap second is expected to create many difficulties.

Changing the rules for UTC to loosen its coupling to UT1 has been extensively discussed since about 2000 (refs. 2,3,44,45). One possibility would be to have larger discontinuities at infrequent but regular intervals; as the Julian calendar showed, an algorithmic procedure is much easier to manage than an irregular one. In November 2022, the CGPM (General Conference on Weights and Measures) resolved that the maximum difference allowed for UTC-TAI should be increased before 2035 (https://www.bipm.org/en/cgpm-2022/resolution-4/). The analysis presented here, showing a strong possibility of a negative second within this decade, suggests a more immediate change to the rules for UTC: never allow a negative discontinuity. Figure 2 suggests that, at the 1-s level, differences between UT1 and a UTC without leap seconds can be predicted at least a year in advance; this will be valuable in supporting any timescales[46] that must be closely coupled to the rotation of Earth.

The acceleration in PDMT, which suggests a steady slowing of the core, makes the likelihood of a future leap second more obvious. But this acceleration has also postponed the negative leap-second problem. Figure 2d shows an alternate history in which the PDMT acceleration did not occur; in this case, the first negative leap second would happen 3 years earlier. Changes in the core have made Δ_ω close enough to zero that global warming and global timekeeping have become inextricably linked and may be more so in the future.

Online content

Any methods, additional references, Nature Portfolio reporting summaries, source data, extended data, supplementary information,

acknowledgements, peer review information; details of author contributions and competing interests; and statements of data and code availability are available at https://doi.org/10.1038/s41586-024-07170-0.

1. McCarthy, D. D. & Seidelmann, P. K. *Time: From Earth Rotation to Atomic Physics* (Cambridge Univ. Press, 2018).
2. Levine, J., Tavella, P. & Milton, M. Towards a consensus on a continuous coordinated universal time. *Metrologia* **60**, 014001 (2023).
3. Nelson, R. A. et al. The leap second: its history and possible future. *Metrologia* **38**, 509–529 (2001).
4. Loomis, B. D., Rachlin, K. E. & Luthcke, S. B. Improved Earth oblateness rate reveals increased ice sheet losses and mass-driven sea level rise. *Geophys. Res. Lett.* **46**, 6910–6917 (2019).
5. Cheng, M. & Ries, J. C_{20} and C_{30} variations from SLR for GRACE/GRACE-FO science applications. *J. Geophys. Res. Solid Earth* **128**, e2022JB025459 (2023).
6. Lombardi, M. A., Novick, A. N., Neville-Neil, G. & Cooke, B. Accurate, traceable, and verifiable time synchronization for world financial markets. *J. Res. Natl Inst. Stand. Technol.* **121**, 436–463 (2016).
7. Addomine, M. in *A General History of Horology* (eds Turner, A. et al.) 137–152 (Oxford Univ. Press, 2022).
8. Glennie, P. & Thrift, N. *Shaping the Day: A History of Timekeeping in England and Wales 1300–1800* (Oxford Univ. Press, 2009).
9. Kinns, R. Visual time signals for mariners between their introduction and 1947: a new perspective. *J. Astron. Hist. Herit.* **25**, 601–713 (2022).
10. Ellis, W. Lecture on the Greenwich system of time signals. *Horol. J.* **7**, 85–91, 97–102, 109–114, 121–124 (1865).
11. Nye, J. & Rooney, D. in *A General History of Horology* (eds Turner, A. et al.) 495–531 (Oxford Univ. Press, 2022).
12. Nelson, G. K., Lombardi, M. A. & Okayama, D. T. NIST time and frequency radio stations: Www, WWVH, and WWVB. NIST Special Publication 250-67 (U.S. Department of Commerce, 2005).
13. Agnew, D. C. Time marks and clock corrections: a century of seismological timekeeping. *Seismol. Res. Let.* **91**, 1417–1429 (2020).
14. Bullard, E. C. An atomic standard of frequency and time interval: definition of the second of time. *Nature* **176**, 282 (1955).
15. Guinot, B. & Arias, E. F. Atomic time-keeping from 1955 to the present. *Metrologia* **42**, S20–S30 (2005).
16. Leschiutta, S. The definition of the 'atomic' second. *Metrologia* **42**, S10–S19 (2005).
17. Munk, W. H. & McDonald, G. *The Rotation of the Earth: A Geophysical Discussion* (Cambridge Univ. Press, 1960).
18. Ray, R. D. & Erofeeva, S. Y. Long-period tidal variations in the length of day. *J. Geophys. Res.* **119**, 1498–1509 (2014).
19. Gross, R. S. in *Treatise on Geophysics: Geodesy* (ed. Herring, T. A.) 215–261 (Elsevier, 2015).
20. Haigh, I. D. et al. The tides they are a-changin': a comprehensive review of past and future nonastronomical changes in tides, their driving mechanisms, and future implications. *Rev. Geophys.* **58**, e2018RG000636 (2020).
21. Williams, J. G. & Boggs, D. H. Secular tidal changes in lunar orbit and Earth rotation. *Celest. Mech. Dyn. Astron.* **126**, 89–129 (2016).
22. Whitehouse, P. L. Glacial isostatic adjustment modelling: historical perspectives, recent advances, and future directions. *Earth Surf. Dynam.* **6**, 401–429 (2018).
23. Peltier, W. R., Wu, P. P.-C., Argus, D. F., Li, T. & Velay-Vitow, J. Glacial isostatic adjustment: physical models and observational constraints. *Rep. Prog. Phys.* **85**, 096801 (2022).
24. Mitrovica, J. et al. Reconciling past changes in Earth's rotation with 20th century global sea-level rise: Resolving Munk's enigma. *Sci. Adv.* **1**, e1500679 (2015).
25. Kim, A. J. et al. Ice age effects on the satellite-derived $\dot{J}_2$ datum: mapping the sensitivity to 3D variations in mantle viscosity. *Earth Planet. Sci. Lett.* **581**, 117372 (2022).
26. Seago, J. H. in *Requirements for UTC and Civil Timekeeping on Earth* (eds Seago, J. H. et al.) 107–125 (Univelt, American Astronautical Society, 2013).
27. Cheng, M., Tapley, B. & Ries, J. Deceleration in the Earth's oblateness. *J. Geophys. Res. Solid Earth* **118**, 740–747 (2013).
28. Lau, H. C. P. et al. Inferences of mantle viscosity based on ice age data sets: Radial structure. *J. Geophys. Res. Solid Earth* **121**, 6991–7012 (2016).
29. Mitrovica, J. X. & Peltier, W. R. Present-day secular variations in the zonal harmonics of Earth's geopotential. *J. Geophys. Res. Solid Earth* **98**, 4509–4526 (1993).
30. Cox, C. M. & Chao, B. F. Detection of a large-scale mass redistribution in the terrestrial system since 1998. *Science* **297**, 831–833 (2002).
31. Roy, K. & Peltier, W. R. GRACE era secular trends in Earth rotation parameters: a global scale impact of the global warming process? *Geophys. Res. Lett.* L10306 (2011).
32. Fox-Kemper, B. et al. in *Climate Change 2021: The Physical Science Basis. Sixth Assessment Report of the Intergovernmental Panel on Climate Change* (eds Masson-Delmotte, V. et al.) 1211–1362 (Cambridge Univ. Press, 2021).
33. Barnoud, A. et al. Revisiting the global mean ocean mass budget over 2005–2020. *Ocean Sci.* **19**, 321–334 (2023).
34. Wilson, C. *The Hill-Brown Theory of the Moon's Motion: Its Coming-to-Be and Short-Lived Ascendancy (1877–1984)* (Springer, 2010).
35. Kono, M. (ed.) *Treatise on Geophysics, Vol. 5: Geomagnetism* (series ed. Schubert, G.) (Elsevier, 2015).
36. Olson, P. (ed.) *Treatise on Geophysics, Vol. 8: Core Dynamics* (series ed. Schubert, G.) (Elsevier, 2015).
37. Langbein, J. Methods for rapidly estimating velocity precision from GNSS time series in the presence of temporal correlation: A new method and comparison of existing methods. *J. Geophys. Res. Solid Earth* **125**, e2019JB019132 (2020).
38. Constable, C. & Constable, S. A grand spectrum of the geomagnetic field. *Phys. Earth Planet. Inter.* **344**, 107090 (2023).
39. Stephenson, F. R., Morrison, L. V. & Hohenkerk, C. Y. Measurement of the Earth's rotation: 720 BC to AD 2015. *Proc. R. Soc. A* **472**, 20160404 (2016).
40. Huber, P. J. Modeling the length of day and extrapolating the rotation of the Earth. *J. Geod.* **80**, 283–303 (2006).
41. Morrison, L. V., Stephenson, F. R., Hohenkerk, C. Y. & Zawilski, M. Addendum 2020 to 'Measurement of the Earth's rotation: 720 BC to AD 2015'. *Proc. R. Soc. A* **477**, 20200776 (2021).
42. Bell, S. A., Bangert, J. A. & Kaplan, G. H. in *The History of Celestial Navigation: Rise of the Royal Observatory and Nautical Almanacs* (eds Seidelmann, P. K. & Hohenkerk, C. Y.) 263–311 (Springer, 2020).
43. Burnicki, M. in *Requirements for UTC and Civil Timekeeping on Earth* (eds Seago, J. H. et al.) 35–46 (Univelt, American Astronautical Society, 2013).
44. Seidelmann, P. K. & Seago, J. H. Time scales, their users, and leap seconds. *Metrologia* **48**, S186–S194 (2011).
45. Seago, J. H., Seaman, R. L., Seidelmann, P. K. & Allen, S. L. (eds) *Requirements for UTC and Civil Timekeeping on Earth* (Univelt, American Astronautical Society, 2013).
46. Birth, K. in *Law and Time* (eds Benyon-Jones, S. M. & Grabham, E.) 196–211 (Routledge, 2018).

Methods

The J_2 data in Fig. 1 was derived from the original by adding a trend of -0.35×10^{-10} yr^{-1}, which is the rate of change from 1976 to 1991. It was then seasonally adjusted[47], with smoothing over 1 year. A quadratic function of time was fit over the entire time span by weighted least squares, using the errors provided with the data; this quadratic is $0.128 \times 10^{-11}(t - 1985.9)^2 - 0.21 \times 10^{-10}$, where t is the date.

In Fig. 2, the rate of 0.35×10^{-10} yr^{-1} has been reapplied to the two PDMT series. The straight-line fit to the series in Fig. 2c was made using a procedure[37] that allows for autocorrelation in this series. The slope of this line is $-1.1 \pm 0.4 \times 10^{-10}$ yr^{-1}; its large standard error is a consequence of temporal correlation in the series[48].

Data availability

The J_2 data are C20LongTerm.txt, downloaded from https://filedrop.csr.utexas.edu/pub/slr/degree_2/ on 25 October 2023. The Earth rotation data are eopc0420.1962-now, downloaded from https://datacenter.iers.org/products/eop/long-term/c04_20/ on 24 October 2023. The atmospheric angular momentum data are from https://datacenter.iers.org/products/geofluids/atmosphere/aam/GGFC2010/AER/, downloaded on 1 February 2023. Other parameters are taken from the papers referenced. Source data are provided with this paper.

Code availability

The code for analysing the residual series, est.noise v.1.2, was downloaded from https://github.com/langbein-usgs on 25 June 2023. The seasonal-adjustment code stl was slightly modified from a version downloaded from https://netlib.org/a/ in June 2008.

47. Cleveland, R. B., Cleveland, W. S., McRae, J. E. & Terpenning, I. STL: a seasonal-trend decomposition procedure based on loess. *J. Off. Stat.* **6**, 3–73 (1990).
48. Johnson, H. & Agnew, D. C. Monument motion and measurements of crustal velocities. *Geophys. Res. Lett.* **22**, 2905–2908 (1995).

Acknowledgements I thank R. Ray, L. Morrison, A. Borsa and J. Mitrovica for their comments.

Competing interests The author declares no competing interests.

Additional information
Correspondence and requests for materials should be addressed to Duncan Carr Agnew.
Peer review information *Nature* thanks Jerry Mitrovica and the other, anonymous, reviewer(s) for their contribution to the peer review of this work.